

University of Nebraska - Lincoln

DigitalCommons@University of Nebraska - Lincoln

Xiao Cheng Zeng Publications

Published Research - Department of Chemistry

9-22-2003

Effect of polarizability of halide anions on the ionic salvation in water clusters

S. Yoo

University of Nebraska-Lincoln

Y.A. Lei

University of Nebraska-Lincoln

Xiao Cheng Zeng

University of Nebraska-Lincoln, xzeng1@unl.edu

Follow this and additional works at: <https://digitalcommons.unl.edu/chemzeng>

 Part of the [Chemistry Commons](#)

Yoo, S.; Lei, Y.A.; and Zeng, Xiao Cheng, "Effect of polarizability of halide anions on the ionic salvation in water clusters" (2003). *Xiao Cheng Zeng Publications*. 32.

<https://digitalcommons.unl.edu/chemzeng/32>

This Article is brought to you for free and open access by the Published Research - Department of Chemistry at DigitalCommons@University of Nebraska - Lincoln. It has been accepted for inclusion in Xiao Cheng Zeng Publications by an authorized administrator of DigitalCommons@University of Nebraska - Lincoln.

Effect of polarizability of halide anions on the ionic solvation in water clusters

S. Yoo, Y. A. Lei,^{a)} and X. C. Zeng^{b)}

Department of Chemistry, University of Nebraska-Lincoln, Lincoln, Nebraska 68588

(Received 17 June 2003; accepted 25 June 2003)

Molecular dynamics simulation has been performed to study the effect of the polarizabilities of model anions on the ionic solvation in water clusters. The primary focus is given to the surface versus interior solvation behavior of the anions. To this end, various combinations of polarizable/nonpolarizable water and anion models were considered. Using the nonpolarizable TIP4P water with polarizable Cl^- and Br^- models, the Cl^- is fully solvated inside the $(\text{H}_2\text{O})_{60}$ cluster, whereas the Br^- is partially solvated at the surface of the cluster. However, when the polarizability of the Br^- is turned off, the “ Br^- ” anion is fully solvated. Using the polarizable Dang–Chang water, both Cl^- and Br^- reside at the surface of $(\text{H}_2\text{O})_{60}$ as well as $(\text{H}_2\text{O})_{500}$ clusters, consistent with the finding of Stuart and Berne [J. Phys. Chem. **100**, 11934 (1996)] based on the polarizable TIP4P-FQ water with the polarizable Drude halide model. When the polarizabilities of the halide anions are turned off, the smaller size “ Cl^- ” anion is fully solvated in the interior of the Dang–Chang water cluster, whereas the larger “ Br^- ” anion is still partially solvated at the surface of the cluster, indicating the importance of the anion-size effect. We have also calculated the free energy change for the Cl^- moving from the center of a lamella water slab to the surface. The free-energy change is on the order of 1 kcal/mol, indicating that the Cl^- can easily access the surface region of the Dang–Chang water slab. © 2003 American Institute of Physics. [DOI: 10.1063/1.1601609]

I. INTRODUCTION

It is known that chemical reactions between molecular gases such as Cl_2 and Br_2 and heavy halide anions Cl^- and Br^- in solution occur in the upper atmosphere.^{1–3} Since most reactions take place at the liquid surface, availability of halide anions at the liquid surface is expected. Experimental measurements of the surface potential of NaCl solution have shown that the concentration of Cl^- is higher than that of Na^+ near the solution surface.⁴ Photoelectron spectroscopy experiments have revealed that the I^- anion typically resides at the surface of water cluster having 60 water molecules or less, and that I^- is not as fully solvated as Br^- and Cl^- .⁵ A recent vibrational-predissociation-spectrum measurement for the $\text{Cl}^-(\text{CH}_3\text{OH})_n$ cluster ($n \leq 12$) suggested that large anion polarizability is a key factor leading to the surface solvation.⁶ Despite many experiments on ionic solvations, direct evidences on structural characteristics of anionic solvation are still limited.

Theoretical and computational studies on halide anionic solvation have been mostly focused on the development of potential parameters to account for anion–water interactions,^{7–11} and on the characterization of structural properties of small aqueous ionic clusters^{12–22} as well as ions in water slabs.^{21,23–25} For small clusters of $\text{Cl}^-(\text{H}_2\text{O})_n$ ($n \leq 14$), several molecular dynamics (MD) simulations have shown that the Cl^- always locates favorably at the surface of the water clusters, regardless the use of the polarizable or nonpolarizable water models.^{15,16} In the case of midsize wa-

ter clusters (e.g., $20 \leq n \leq 500$), however, the solvation behavior of Cl^- appears quite sensitive to the polarizability of the water model.¹⁵ For example, Stuart and Berne^{20,21} have found that the Cl^- generally locates inside nonpolarizable water clusters but prefers to reside at the surface of polarizable water clusters even with the water cluster size as large as 255. They attributed to the latter surface solvation behavior to the large effective dipole moment resulted by the use of the polarizable water model. They pointed out that the large effective dipole moment can strengthen the hydrogen bond network. Thus, to keep the hydrogen-bond network more intact the anion has to be excluded from the interior of the water cluster.^{20,21} The free energy of ionic solvation has been calculated via MD simulation for water slab systems.^{23,24} Wilson and Pohorille found that when the nonpolarizable TIP4P water model is employed, anions can be fully solvated in the slab. The free energy change for the Cl^- moving from the center of the slab to the surface amounts to 4.5 kcal/mol.²⁴

Given the fact that the polarizability of water can have significant effect on the behavior of anionic solvation, it is interesting to see whether the polarizability of anion would have a similar effect. Because the polarizability of most elemental particles increases with their size, the polarization effect can compete with the size effect. For example, within the halide group, the polarizability of F^- is the smallest. In this case, the polarization effect on the solvation of F^- in water clusters is minute. In fact, it is known that F^- can be fully solvated even in small-size water clusters because of the small size of F^- anion as well as the strong electrostatic interaction between F^- and water molecules. The larger ha-

^{a)}Department of Computer Science and Engineering.

^{b)}Electronic mail: xzeng1(a)unl.edu

TABLE I. Potential energy parameters, charges, and polarizabilities for water molecules.

	TIP4P	Dang–Chang
ϵ (kcal/mol)	0.1550	0.1825
σ (Å)	3.1536	3.2340
θ_{HOH} (deg)	104.52	104.50
r_{OH} (Å)	0.9572	0.9572
r_{OM} (Å)	0.150	0.215
$q_{\text{H}}(e)$	0.52	0.519
α (Å ³)	0.000	1.444

lide anion such as (I^-) tends to have more chances to access the surface region of the water cluster than the smaller ones (i.e., Cl^-). This is because by residing at the surface of the clusters it can allow more hydrogen-bonding interactions among water molecules. In this study, we will present molecular dynamics evidences that the polarization effect of anions can also play a significant role, in some cases can be more significant than the ion-size effect, in the interior versus surface solvation. Previous molecular dynamics simulations^{20,21} have indicated that the polarizability of halide ions have minor effect on the structure and dynamics of water clusters. Those studies were based on very accurate parameterization of the halide ion, both polarizable and non-polarizable models, by fitting to the experimental value of the first peak of the pair correlation function, the heterodimer bond length as well as to the bond energy of *ab initio* calculation. Therefore, those simulations represent a more realistic description of the halide ionic solvation in water clusters. In this study, we give more attention to the general physical trend of interior versus surface solvation by systemically changing the polarizability and size parameters of model anions. As a consequence the modified models no longer represent a realistic description of the halide ion–water interaction. However, the systematic changing of the anion parameters allows us to obtain more generic features of the anionic solvation. Another goal in this study is to evaluate the free energy change required to move the anion toward the interface of a water slab. In Sec. II, various water and halide ion models are illustrated. The simulation details are also described in Sec. II. The results and discussions are given in Sec. III and the conclusion is in Sec. IV.

II. MODELS AND SIMULATION DETAILS

The nonpolarizable water model considered in this study is the TIP4P model,⁹ and the polarizable water model is the Dang–Chang model.²⁶ Both potential models have four interaction sites: two hydrogen (H) sites, one oxygen (O) site, and one virtual site (M). Only the oxygen site has Lennard-Jones potential parameters. The virtual site (M) has a negative charge of $-2q_{\text{H}}$, where q_{H} is the positive charge on the two hydrogen sites. The TIP4P potential model is nonpolarizable, and thus one can view that it has zero polarizability $\alpha=0.0$ Å.³ The potential parameters of the TIP4P and Dang–Chang water models are summarized in Table I.

The potential energy U_{tot} of the simulation system can be written as the sum of the additive pairwise interaction

TABLE II. Potential energy parameters of the polarizable halide anions.

	Cl^- (Ref. 12)	Br^- (Ref. 19)
ϵ (kcal/mol)	0.1	0.1
σ (Å)	4.321	4.603
α (Å ³)	3.250	4.533

energy U_{pair} and the nonadditive polarizable interaction energy U_{pol} , i.e.,

$$U_{\text{tot}} = U_{\text{pair}} + U_{\text{pol}}. \quad (1)$$

The pairwise part U_{pair} is given by the sum of the Lennard-Jones and Coulomb interactions,

$$U_{\text{pair}} = \sum_i \sum_{j>i} \left(4\epsilon_{ij} \left[\left(\frac{\sigma_{ij}}{r_{ij}} \right)^{12} - \left(\frac{\sigma_{ij}}{r_{ij}} \right)^6 \right] + \frac{q_i q_j}{r_{ij}} \right). \quad (2)$$

Here, r_{ij} is the distance between site i and site j in different molecules, q_i is the charge of site i , σ and ϵ are the Lennard-Jones parameters satisfying the combining rules $\sigma_{ij} = \sqrt{\sigma_{ii}\sigma_{jj}}$ and $\epsilon_{ij} = \sqrt{\epsilon_{ii}\epsilon_{jj}}$. The nonadditive polarizable energy U_{pol} is given by

$$U_{\text{pol}} = -\frac{1}{2} \sum_i \boldsymbol{\mu}_i \cdot \mathbf{E}_i^0, \quad (3)$$

where \mathbf{E}_i^0 is the electric field at the site i , produced by the fixed charges in other molecules

$$\mathbf{E}_i^0 = \sum_{j \neq i} \frac{q_j \mathbf{r}_{ij}}{r_{ij}^3}, \quad (4)$$

and $\boldsymbol{\mu}_i$ is the induced dipole moment at the site i . $\boldsymbol{\mu}_i$ is expressed as

$$\boldsymbol{\mu}_i = \alpha_i \mathbf{E}_i = \alpha_i \left[\mathbf{E}_i^0 + \sum_{j \neq i} \mathbf{T}_{ij} \cdot \boldsymbol{\mu}_j \right], \quad (5)$$

where \mathbf{E}_i is the total electric field at the site i , α_i is the molecular polarizability of the molecule i , and \mathbf{T}_{ij} is the dipole tensor,

$$\mathbf{T}_{ij} = \frac{1}{r_{ij}^3} \left(\frac{3\mathbf{r}_{ij}\mathbf{r}_{ij}}{r_{ij}^2} - \mathbf{I} \right), \quad (6)$$

where \mathbf{I} is the unit tensor. We used the standard iterative self-consistent field procedure to evaluate the induced dipole moment with Eq. (5). The iterations are continued until the maximum difference in the induced dipole moment between successive iterations is less than 0.0001 D/molecule. The calculation of the forces due to the charge–dipole and dipole–dipole interactions follows that of Ahlström *et al.*²⁷ The parameters of polarizable halide anion Cl^- and Br^- are given in Table II. The Cl^- model is that developed by Dang *et al.*¹² and Br^- by Berkowitz and co-workers.¹⁹

In the MD simulation of anion–water clusters, no cutoff distance was used. The simulation cell has the dimensions 50 Å × 50 Å × 50 Å for $(\text{H}_2\text{O})_{60}$ and 100 Å × 100 Å × 100 Å for $(\text{H}_2\text{O})_{500}$. We fixed the position of one water molecule at the center of the simulation cell but allowed it to rotate. For the water slab, the system consists of 639 water molecules and 1

Cl^- ion. The system cell has the dimensions $24.868 \text{ \AA} \times 24.868 \text{ \AA} \times 85.0 \text{ \AA}$. The z -axis is set normal to the water slab. Periodic boundary conditions were applied in all directions. For the MD simulation of the water slab system, a cutoff distance $r_c = 12.0 \text{ \AA}$ was used, beyond which the intermolecular interaction was considered to be zero. Note that Berkowitz and co-workers have studied the effect of different treatments of long-range forces on the dynamics of ions in aqueous solutions.²⁸ They showed that simple truncation can give results similar to those based on the Ewald sum or reaction field method.

The standard quaternion technique was employed to calculate the angular momentum and the torque. The predictor-corrector method was used to solve the equations of motion. The MD simulations were carried out in the canonical (constant NVT) ensemble and the modified Nosé–Andersen's method was used to maintain the constant-temperature condition.²⁹ A time step of $\Delta\tau = 1 \text{ fs}$ was utilized in the MD simulations. After 500 ps equilibration run for the clusters (100 ps for the slab), data were accumulated for every ten MD time steps over the period of 1 ns production run.

III. RESULTS AND DISCUSSIONS

A. Nonpolarizable TIP4P water clusters

To examine whether an anion is fully solvated inside a water cluster or partially solvated at the surface, we calculated the normalized density profile $\rho(r_{\text{com}})$ of the oxygen of water molecules and that of the anion as a function of the radial distance r_{com} from the center of mass (COM) of water cluster. The mass of the anion was excluded in the calculation of the COM. Figures 1(a) and 1(b) show the density profiles of the polarizable Cl^- and Br^- , as well as those of the oxygen sites of water molecules for the $\text{Cl}^-(\text{H}_2\text{O})_{60}$ and $\text{Br}^-(\text{H}_2\text{O})_{60}$ systems. The Cl^- is fully solvated inside the water cluster as shown in Fig. 1(a), whereas the Br^- appears to reside near the surface of the cluster as shown in Fig. 1(b). Since the Br^- has both a larger size and polarizability than Cl^- , we also performed MD simulation with several artificial “ Cl^- ” and “ Br^- ” models [Figs. 1(c)–1(e)] for the purpose of separating the ion-size effect from the polarization effect. In Fig. 1(c), we plot the density profile of the artificial “ Cl^- ” anion which has the size and mass of Cl^- but the polarizability of Br^- . This anion is no longer fully solvated inside the cluster but partially solvated at the surface of the cluster, somewhat similar to the behavior of the Br^- [Fig. 1(b)]. Figure 1(d) shows the density profile of the artificial “ Br^- ” anion having the size and mass of Br^- but the polarizability of Cl^- . It demonstrates that the anion is mostly solvated in the interior of the cluster but can occasionally reside at the surface of the cluster. These density-profile results suggest that the polarizability of anion can play a significant role in the interior versus surface solvation, at least for the size range of the anions considered. Moreover, it appears that the anion-size effect can be negligible if both the anion and the water models are nonpolarizable. To confirm this conclusion, in Fig. 1(e), we plot the density profile of the artificial “ Br^- ” anion having zero polarizability. Clearly, the anion is always fully solvated inside the water cluster even

the anion has the size of Br^- . Note again that by turning off the polarizability of Br^- , the model itself no longer represents a realistic model for Br^- . As an independent test, we employed another nonpolarizable Br^- model¹⁹ ($\sigma = 5.154 \text{ \AA}$ and $\epsilon = 0.017 \text{ kcal/mol}$). Again, Fig. 1(f) shows that the nonpolarizable Br^- is fully solvated in the TIP4P water cluster.

The density profiles such as those shown in Figs. 1(a), 1(e), and 1(f) provide a clear-cut indication that the anion maintains fully solvated during the production MD run, while those shown in Fig. 1(b) indicate that the anion always locates at the surface of the water cluster. However, the density profiles such as those shown in Figs. 1(c) and 1(d) reveal that both surface and interior solvation can exist. We find that a quantitative single-parameter indicator which can be used to measure the degree of interior solvation (or surface solvation) is the height of the second peak of the ion–oxygen pair correlation function $g_{io}(r)$ (where r is the distance between the ion and the oxygen sites). This is because the second peak of $g_{io}(r)$ can provide a semiquantitative measure of the number of solvent molecules in the second solvation shell about the ion. In Figs. 1(g) and 1(h) we plot $g_{io}(r)$ for the systems considered in Figs. 1(a)–1(f). In both figures, the curves which display the highest and lowest second peak can be viewed as the reference curves since the corresponding cluster systems exhibit clear-cut interior and surface solvation behavior. Those systems whose $g_{io}(r)$ curve has the second peak placed in between the reference curves are expected to show both interior and surface solvation behavior. The dominant solvation behavior is correlated to the height of the second peak of $g_{io}(r)$. If the height is greater than 1.2, the interior solvation should be the dominant one; if the height is lower than 0.8, the surface solvation should be the dominant one; between 0.8 and 1.2, both interior and surface solvation can exist. The higher of the height of the second peak, the greater degree of the interior solvation in the ion-water cluster. As an example, the height of the second peak of the $g_{io}(r)$ curve for the “ Br^- ” ($\alpha = \alpha_{\text{Cl}^-}$) system is about 1.1 [in both Figs. 1(g) and 1(h)]. Thus, for this system, the interior solvation will occur for the most time whereas the surface solvation will occur occasionally. Indeed, by inspecting snapshots of the cluster over a period of 1 ns, we find that most snapshots shows the interior solvation [Fig. 2(a)], whereas a few snapshots show the surface solvation [Fig. 2(b)].

B. Polarizable Dang–Chang water clusters

In Figs. 3(a) and 3(b), we plot the density profiles of the polarizable Cl^- and Br^- as well as those of oxygen sites of the polarizable Dang–Chang water clusters having 60 water molecules. These plots show that the polarizability of water molecules does have major effect on the solvation propensities of the halide ions. With the polarizable Dang–Chang model, both Cl^- and Br^- reside at the surface of the water clusters, a result consistent with the previous finding that including polarization effect in water can significantly change the anionic solvation behavior.^{15,20} As mentioned above, the smaller ion Cl^- is always fully solvated inside the midsize TIP4P (nonpolarizable) water clusters. On the other

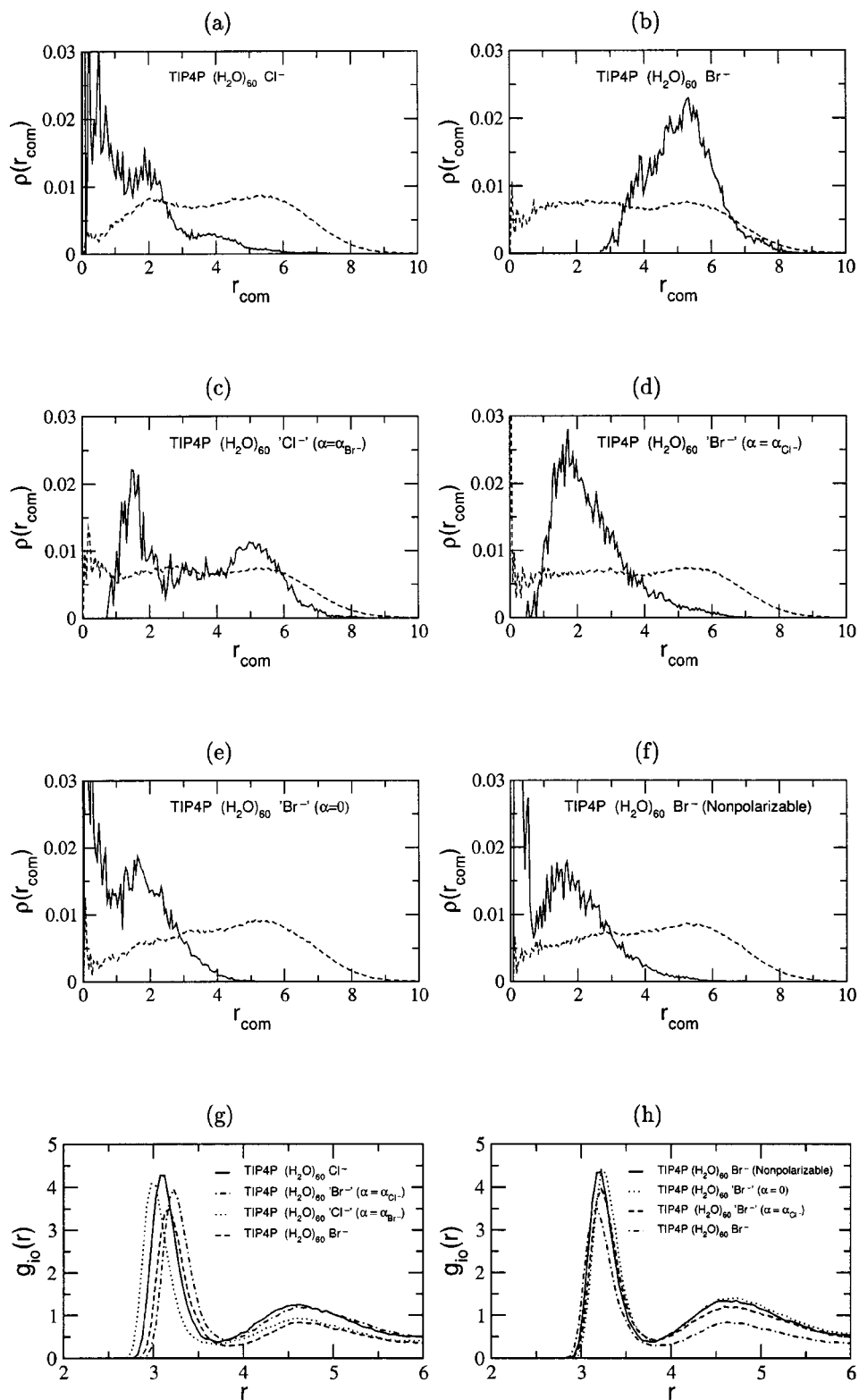


FIG. 1. (a)–(f) The normalized density profiles of the anion (solid lines) and oxygen sites (dashed lines) of nonpolarizable TIP4P water clusters having 60 water molecules: (a) polarizable Cl⁻, (b) polarizable Br⁻, (c) the artificial “Cl⁻” having the polarizability of the Br⁻, (d) the artificial “Br⁻” having the polarizability of the Cl⁻, (e) the artificial “Br⁻” having zero polarizability, and (f) the nonpolarizable model of Br⁻ (Ref. 19). r_{com} is the distance from the anion or oxygen to the center of the mass of the water cluster (excluding the anion). (g)–(h) The anion–oxygen pair correlation functions for the anion–water systems considered in (a)–(f). The system temperature was set at 240 K. r_{com} and r is in units of Å.

hand, as shown in Figs. 3(c) and 3(d), when the polarizabilities of both halide ions are turned off, both anions withdraw from the surface to the interior of the clusters. This result demonstrates the polarizability of anion can also play a significant role in the surface versus interior solvation. In Fig. 3(e), we plot the pair correlation function $g_{io}(r)$ for the anion–water systems shown in Figs. 3(a)–3(d). Again, we find that the height of the second peak of $g_{io}(r)$ curves cor-

relates well with the predominant solvation behavior as discussed above. For example, in Fig. 3(e), the second peak of $g_{io}(r)$ for the artificial “Cl⁻” ($\alpha=0$) system is greater than 1.2, indicating that the anion should be fully solvated inside the Dang–Chang water cluster. However, in Fig. 3(e), the second peak of $g_{io}(r)$ for the Br⁻ system is slightly less than 0.8, indicating that the anion should always reside at the surface of the Dang–Chang cluster.

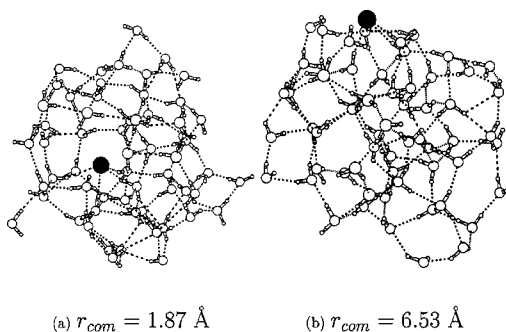


FIG. 2. Two MD snapshots of the anion–water cluster shown in Fig. 1(d). The bigger black sphere represents the artificial “Br[−]” ion having the polarizability of the Cl[−]. In snapshot (a), the anion is fully solvated ($r_{com} = 1.87 \text{ \AA}$); in snapshot (b) the anion is located at the surface of the cluster ($r_{com} = 6.53 \text{ \AA}$).

Having shown that the Cl[−] and Br[−] favor to reside at the surface of the Dang–Chang water clusters with 60 water molecules, a question arises: Is it possible for the halide ions to be fully solvated inside larger Dang–Chang water clusters? To examine this possibility, we performed the MD

simulation of halide ion/water clusters having 500 water molecules. Figures 4(a) and 4(b) show the density profiles of Cl[−] and Br[−]. Even with this size of water cluster, the Br[−] still locates mostly at the surface of the cluster [Fig. 4(b)]. However, the density profile of the smaller size Cl[−] anion [Fig. 4(a)] shows features qualitatively different from those of Br[−] [Fig. 4(b)]. By inspecting the snapshots in the production run, we find that the Cl[−] can occasionally access the interior of the cluster (see Fig. 5). Based on this result, we speculate that the Cl[−] may be fully solvated by a much larger water cluster (see next section). To separate the ion-size effect from the polarization effect, we plot in Fig. 4(c) the density profile of the “Br[−]” anion having the polarizability of Cl[−] ion. Thus, the differences in the density profile between Figs. 4(a) and 4(c) must be due to the ion-size effect. Such differences can be also seen in Fig. 4(f), where it shows that the height of the second peak of $g_{io}(r)$ curve for the Cl[−] water cluster is higher than that for the “Br[−]” ($\alpha = \alpha_{Cl^-}$) water cluster, indicating the latter system should exhibit a greater degree of surface solvation due to the larger ion size. To summarize, anions with a larger size should have

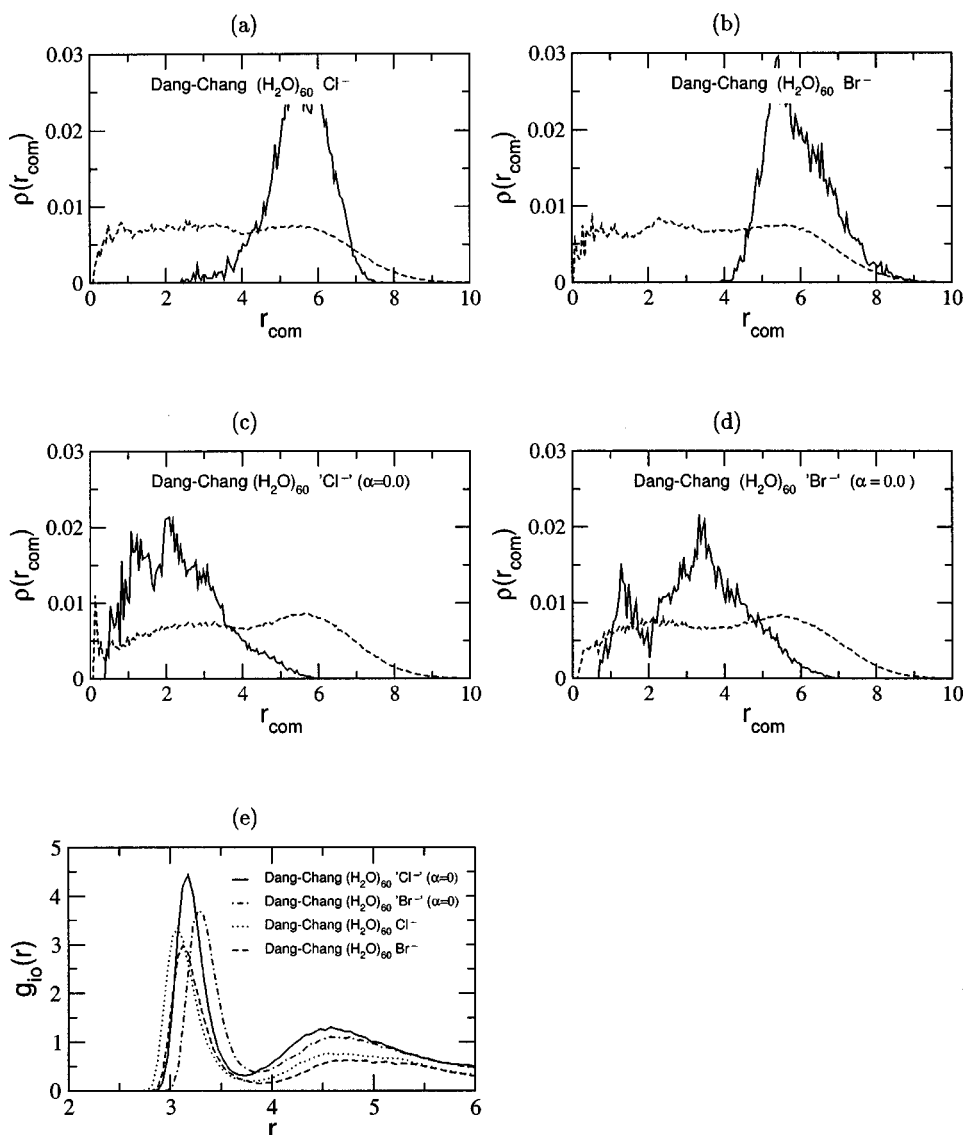


FIG. 3. (a)–(d) The normalized density profiles of the anion (solid lines) and oxygen sites (dashed lines) of Dang–Chang water cluster having 60 water molecules: (a) polarizable Cl[−], (b) polarizable Br[−], (c) the artificial “Cl[−]” having zero polarizability, and (d) the artificial “Br[−]” having zero polarizability. (e) The anion–oxygen pair correlation functions for the anion–water systems are considered in (a)–(d). The system temperature was set at 240 K.

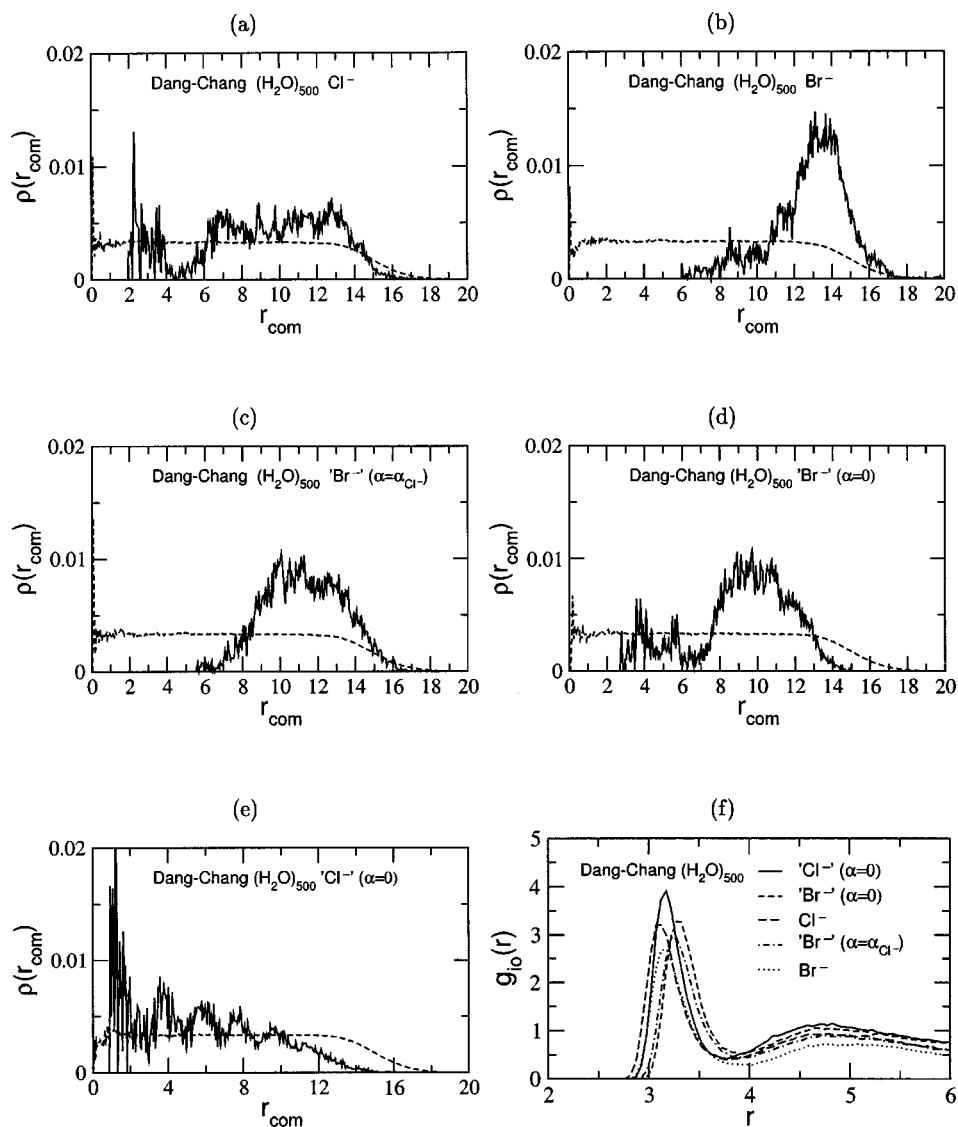
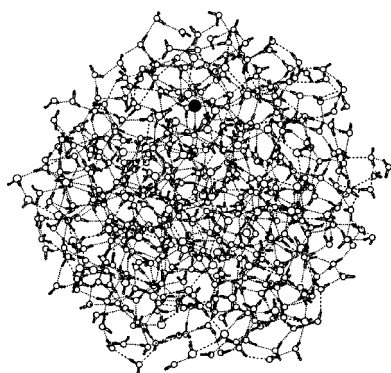


FIG. 4. (a)–(e) The normalized density profiles of the anion (solid lines) and oxygen sites (dashed lines) of the Dang–Chang water cluster having 500 water molecules: (a) polarizable Cl^- , (b) polarizable Br^- , and (c) the artificial “ Br^- ” having the polarizability of Cl^- , (d) the artificial “ Br^- ” having zero polarizability, and (e) the artificial “ Cl^- ” having zero polarizability. (f) The anion–oxygen pair correlation functions for the anion–water systems considered in (a)–(e). The system temperature was set at 298.15 K.

more chances to access the surface region than the smaller ones. Figure 4(d) shows that when the polarizability of the Br^- is turned off, the “ Br^- ” can have much more chances to access the interior of the water cluster. Again, to show the



$$r_{com} = 8.35 \text{ \AA}$$

FIG. 5. A MD snapshot of the anion–water system shown in Fig. 4(a). The bigger black sphere represents the polarizable Cl^- ion. The snapshot shows that the anion is fully solvated ($r_{com} = 8.35 \text{ \AA}$).

ion-size effect, we plot in Fig. 4(e) the density profile of the “ Cl^- ” having zero polarizability. Comparing Fig. 4(e) with Fig. 4(d) one can see that the smaller nonpolarizable “ Cl^- ” is fully solvated inside the Dang–Chang water cluster. Moreover, as discussed above, the height of the second peak of $g_{io}(r)$ curves [Fig. 4(f)] provides a quantitative and consistent measure of the degree of surface solvation in these clusters.

Why is the polarizable Cl^- always fully solvated by the TIP4P water cluster with 60 water molecules? And why cannot the polarizable Br^- be fully solvated by the same water cluster? Why is the “ Cl^- ” with a larger polarizability no longer fully solvated by the TIP4P water cluster? And why can the “ Cl^- ” with zero polarizability be fully solvated by the polarizable Dang–Chang water cluster of the same size? We attempt to offer a simple physical picture to answer some of these questions. Let us consider a two-dimensional point-dipole model for dipolar solvent such as water, as schematically illustrated in Fig. 6. If the anion is nonpolarizable and its size is comparable to the size of the solvent molecule, the anion is mostly likely to be fully solvated by the dipolar solvent molecules with their positive ends pointing toward

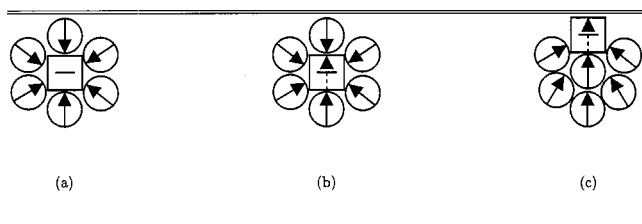


FIG. 6. Schematic plots of two-dimensional anion (open squares)-dipolar particle (open spheres) cluster. (a) The favorable configuration for nonpolarizable anion solvated by dipolar particles with a small dipole moment. The anion tends to be fully solvated in this case. (b) When the anion has a large polarizability and the dipolar particles have a large dipole moment, a large induced dipole (dashed arrow) will result in repulsive dipole-induced dipole interactions which are energetically unfavorable. (c) The more favorable configuration for the system shown in (b). The anion is likely to reside at the surface of the cluster.

the anion. Thus, this simple model provides an explanation why the nonpolarizable anion is fully solvated by mid-sized nonpolarizable water clusters. On the other hand, if the anion is polarizable, an induced dipole moment will be manifested due to the surrounding dipolar molecules. Thus, additional interactions, i.e., the dipole-induced dipole interactions between the dipolar molecules and the anion, should be considered. If the anion polarizability is large, e.g., on the order of the polarizable Br^- , the dipole-induced dipole interaction can be appreciable. As a result, the fully solvated configuration as shown in Fig. 6(b) can become less favorable energetically, compared to that shown in Fig. 6(c). This is due to the unfavorable repulsive dipole-induced dipole interaction between the anion and some surrounding molecules. However, if the anion resides at the surface of the cluster, the repulsive dipole-induced dipole interactions can be largely averted, and more favorable attractive interactions can be resulted.

In summary, the larger the polarizability an anion has, the larger the induced dipole moment will be manifested, and the stronger tendency for the anion to be placed at the surface of the cluster. By the same token, this simple model suggests that the tendency for the anion to move to the surface of the cluster should become stronger if the dipole moment of the surrounding solvent particles is larger. For the polarizable Dang–Chang model, the effective dipole moment (permanent dipole 1.848 D plus the induced dipole) can amount to 2.75 D at the center of large-size clusters and about 2.5 D at the surface of the clusters. Indeed, even the latter value is greater than the permanent dipole moment of TIP4P water molecule (2.18 D). This explains why the polarizable Cl^- prefers to be placed mostly at the surface of the Dang–Chang water cluster, even when the size of the cluster is as large as 500, but this is not the case for the TIP4P water cluster.

C. Free energy change from interior to surface of water slab

In the previous section, we present simulation evidences that even with the size of the Dang–Chang cluster as large as 500, the polarizable Cl^- cannot be fully solvated inside the cluster. A much larger size of the Dang–Chang cluster may

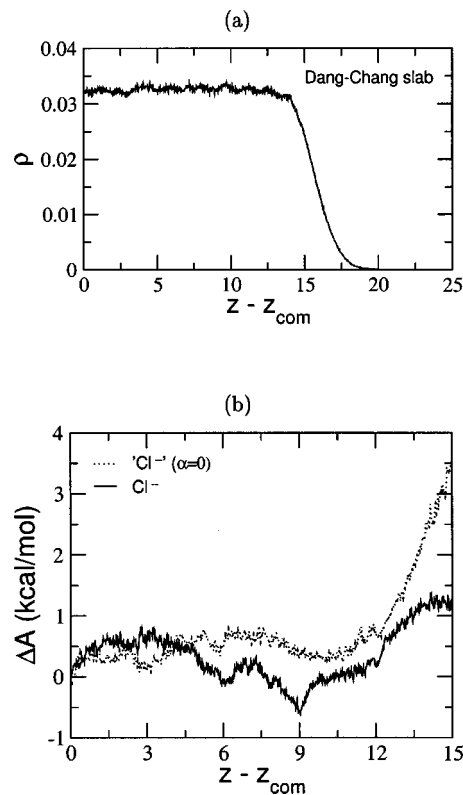


FIG. 7. (a) The density profile of a Dang–Chang water slab, where z_{com} denotes the center of mass of the slab in the z direction. (b) The Helmholtz free energy change ΔA for moving the anion from the point inside the slab ($z - z_{\text{com}} = 0$) to a position ($z - z_{\text{com}} > 0$) toward the surface of the slab.

be required to fully solvate the Cl^- . Note that in some sense, a water slab can be viewed as the infinite-size limit for the water cluster. Therefore, it is possible that the Cl^- can be fully solvated inside the Dang–Chang water slab. To examine this possibility, we calculated the work required to move the Cl^- from the interior of the slab to the surface of slab. The value of this work (or the free energy change) can provide a measure on whether the anion has a good chance to access the surface of the slab (or large-size water clusters). In the simulation, we let the z -axis be normal to the surfaces of the water slab. The free energy change, $\Delta A(z)$, measured from an arbitrary point in the interior of the slab, can be evaluated via the umbrella sampling method. Specifically, we utilized a number of overlapping windows on the z -axis by adding a biasing potential $U_b(z)$ to the slab system,^{24,30} i.e.,

$$U_b(z) = k_l(z_l - z)^{n_l} H(z_l - z) + k_u(z - z_u)^{n_u} H(z - z_u), \quad (7)$$

where $H(x)$ is 0 for $x < 0$ and 1 for $x > 0$. The biasing potential $U_b(z)$ constrains the position of the ion within the window $z_l \leq z \leq z_u$ in the z -direction. We set $k_l = k_u = 1000$ kcal/mol and $n_l = n_u = 3$ in Eq. (7). The free energy change $\Delta A(z)$ can be evaluated from the probability density for finding the ion, $p(z)$, i.e.,

$$\Delta A(z) = -k_B T \ln \frac{p(z)}{p(z_0)}, \quad (8)$$

where k_B is the Boltzmann constant and z_0 is the initial z position of the ion in the slab. Here, we set z_0 to be the center of mass of the slab z_{com} in the z direction. An equimolar surface of the slab locates at $z - z_{\text{com}} = 16.0 \text{ \AA}$ [see Fig. 7(a)]. Boundaries of these windows $[z_l - z_{\text{com}}, z_u - z_{\text{com}}]$ were $[0, 3.0]$, $[3.0, 6.0]$, $[6.0, 9.0]$, $[9.0, 12.0]$, and $[12.0, 15.0]$.

In Fig. 7(b) we plot the Helmholtz free energy change $\Delta A(z - z_{\text{com}})$ for moving the polarizable Cl^- (and the artificial anion “ Cl^- ” with zero polarizability) from the interior of the water slab to the surface of the slab. The free energy change for moving both anions to the near interfacial region $z - z_{\text{com}} \sim 12 \text{ \AA}$ [see Fig. 7(a)] is no larger than 1.0 kcal/mol. Into the interfacial region $z - z_{\text{com}} > 12$, however, we find that it would require a greater work (or a larger free energy change) to move the nonpolarizable “ Cl^- ” ($\alpha=0$) anion than the polarizable Cl^- . This result is consistent with the finite-size cluster results shown in Figs. 3 and 4, that is, the polarizable Cl^- anion is much more easily to access the surface region of the Dang–Chang water clusters. In fact, consider the water slab as an infinite-size water cluster, the free energy change for moving the polarizable Cl^- into the interfacial region (about one molecular layer from the equimolar surface) is on the order of 1 kcal/mol. The Cl^- should have appreciable probability to access the surface region of the water slab. On the other hand, the nonpolarizable “ Cl^- ” ($\alpha=0$) anion should prefer the interior solvation in the Dang–Chang water slab. Note that Wilson and Pohorille have reported the free energy change as large as 4.5 kcal/mol for moving a nonpolarizable Cl^- anion from the center of the TIP4P slab to within one water molecular layer of the interface.²⁴ Again, the relatively large free energy change associated with the nonpolarizable anion and TIP4P model is consistent with the finite-size cluster result, that is, the probability for the nonpolarizable Cl^- to access the surface region of water cluster is much smaller compared to that for the polarizable Cl^- .

IV. CONCLUSION

We have carried out molecular dynamics simulations to study the effect of adding the polarizability to the model halide anions on the ionic solvation in water clusters and in lamella water slabs. Primary focus is given to the surface versus interior solvation behavior of the anions. Key findings in this study can be summarized as follows: First, with the nonpolarizable TIP4P water, we find that the polarizable Cl^- is fully solvated in the interior of $(\text{H}_2\text{O})_{60}$ cluster, whereas the Br^- is partially solvated near the surface of the cluster. However, when the polarizability of the Br^- is turned off, the “ Br^- ” ion becomes fully solvated. We find that the height of the second peak of the anion–oxygen pair correlation function can be a quantitative parameter to measure the degree of the surface (or interior) solvation. Second, with the polarizable Dang–Chang water, we find that both the polarizable Cl^- and Br^- anions prefer to reside at the surface of clusters with 60 and 500 water molecules. This result is consistent with the finding by Stuart and Berne²⁰ who used the polarizable TIP4P-FQ water with the polarizable Drude halide model. When the polarizability of the halide ion is turned off, the smaller size “ Cl^- ” anion is fully solvated

inside the water cluster and the larger size “ Br^- ” shows both surface and interior solvation behavior. We conclude that anions with large polarizability are more likely to reside near the surface of water clusters. Third, we have calculated the free energy change for the Cl^- moving from the center of a Dang–Chang water slab to the surface. The free-energy change is typically on the order of 1 kcal/mol, indicating that the Cl^- has appreciable probability to access the surface region of the Dang–Chang water slab. In addition to the polarization effect, we find that the ion-size effect can be important if the water or the anion has a nonzero polarizability. Larger anions are more likely to reside at the surface of the cluster than the smaller ones. However, if both the water and the anion are nonpolarizable, the size of ion has much less effect on the surface vs interior solvation behavior.

A simple physical picture has been proposed to qualitatively understand some aspects of anion polarizability on the anion solvation behavior in the water clusters. In this picture, the major cause for the surface solvation stems from the avoidance of the repulsive induced-dipole–dipole interactions between the polarizable anion and the surrounding (strongly dipolar) water molecules. This simple picture can explain some anionic solvation features such as why nonpolarizable anions favor interior solvation whereas polarizable anions favor surface solvation. The larger the anion polarizability and the larger the effective dipole moment of the solvent molecules, the more likely the anion exhibits surface solvation. Since the polarizable Dang–Chang molecule has relatively larger effective dipole moments (2.5–2.75 D) compared to the TIP4P water molecule (2.18 D), the polarizable Cl^- should be more easily placed at the surface of the Dang–Chang water cluster, as well as the surface of Dang–Chang water slab. To close, MD simulation of ionic solvation in water clusters can be useful to understand certain aspects of surface chemical reactions between gases and anions in solutions, as a key requirement for surface chemical reactions is the availability of sufficient anions at the liquid surface. In particular, the MD simulation can provide some insightful information to relate the availability of anions at the surface to the polarizability factor of the anions.

ACKNOWLEDGMENTS

The authors thank Dr. V. Warshavsky and Dr. G. T. Gao for valuable discussions. This work is supported by the National Science Foundation and by the Research Computing Facility at the University of Nebraska-Lincoln.

¹J. H. Hu, Q. Shi, P. Davidovits, D. R. Worsnop, M. S. Zahniser, and C. E. Kolb, *J. Phys. Chem.* **99**, 8768 (1995).

²L. Magi, F. Schweitzer, C. Pallares, S. Cherif, P. Mirabel, and C. George, *J. Phys. Chem. A* **101**, 4943 (1997).

³E. M. Knipping, M. J. Lakin, K. L. Foster, P. Jungwirth, D. J. Tobias, R. B. Gerber, D. Dabdub, and B. J. Finlayson-Pitts, *Science* **228**, 301 (2000).

⁴L. J. Jarvis and M. A. Scheiman, *J. Phys. Chem.* **72**, 74 (1968).

⁵G. Markovich, S. Pollack, R. Giniger, and O. Cheshnovsky, *J. Chem. Phys.* **101**, 9344 (1994).

⁶O. M. Cabarcos, C. J. Weinheimer, T. J. Martinez, and J. M. Lisy, *J. Chem. Phys.* **110**, 9516 (1999).

- ⁷J. Chandrasekhar, D. C. Spellmeyer, and W. L. Jorgensen, *J. Am. Chem. Soc.* **106**, 903 (1984).
- ⁸P. Cieplak, T. P. Lybrand, and P. A. Kollman, *J. Chem. Phys.* **86**, 6393 (1987).
- ⁹W. L. Jorgensen, J. Chandrasekhar, J. D. Madura, R. W. Impey, and M. L. Klein, *J. Chem. Phys.* **79**, 926 (1983).
- ¹⁰J. Caldwell, L. X. Dang, and P. A. Kollman, *J. Am. Chem. Soc.* **112**, 9144 (1990).
- ¹¹L. X. Dang, *J. Chem. Phys.* **97**, 2659 (1992).
- ¹²L. X. Dang, J. E. Rice, J. Caldwell, and P. A. Kollman, *J. Am. Chem. Soc.* **113**, 2481 (1991).
- ¹³L. X. Dang and B. C. Garrett, *J. Chem. Phys.* **99**, 2972 (1993).
- ¹⁴L. X. Dang and D. E. Smith, *J. Chem. Phys.* **99**, 6950 (1993).
- ¹⁵L. Perera and M. L. Berkowitz, *J. Chem. Phys.* **95**, 1954 (1991).
- ¹⁶W. L. Jorgensen and D. L. Severance, *J. Chem. Phys.* **99**, 4233 (1993).
- ¹⁷L. Perera and M. L. Berkowitz, *J. Chem. Phys.* **96**, 8288 (1992).
- ¹⁸L. Perera and M. L. Berkowitz, *J. Chem. Phys.* **99**, 4222 (1993).
- ¹⁹L. S. Sremaniak, L. Perera, and M. L. Berkowitz, *Chem. Phys. Lett.* **219**, 377 (1994).
- ²⁰S. J. Stuart and B. J. Berne, *J. Phys. Chem.* **100**, 11934 (1996).
- ²¹S. J. Stuart and B. J. Berne, *J. Phys. Chem. A* **103**, 10300 (1999).
- ²²P. Jungwirth and D. J. Tobias, *J. Phys. Chem. A* **106**, 379 (2002).
- ²³I. Benjamin, *J. Chem. Phys.* **95**, 3698 (1991).
- ²⁴M. A. Wilson and A. Pohorille, *J. Chem. Phys.* **95**, 6005 (1991).
- ²⁵P. Jungwirth and D. J. Tobias, *J. Phys. Chem. B* **104**, 7702 (2000).
- ²⁶L. X. Dang and T.-M. Chang, *J. Chem. Phys.* **106**, 8149 (1997).
- ²⁷P. Ahlström, A. Wallqvist, S. Engström, and B. Jönsson, *Mol. Phys.* **68**, 563 (1989).
- ²⁸L. Perera, U. Essmann, and M. L. Berkowitz, *J. Chem. Phys.* **102**, 450 (1995).
- ²⁹D. C. Rapaport, *The Art of Molecular Dynamics Simulations* (Cambridge University Press, Cambridge, 1997).
- ³⁰D. Chandler, *Introduction to Modern Statistical Mechanics* (Oxford University Press, New York, 1987).